TOPICAL REVIEW — Celebrating 30 Years of *Chinese Physics B*

Research progress of Pt and Pt-based cathode electrocatalysts for proton-exchange membrane fuel cells

Ni Suo(索妮), Longsheng Cao(曹龙生), Xiaoping Qin(秦晓平), and Zhigang Shao(邵志刚)[†]

Fuel-Cell System and Engineering Laboratory, Key Laboratory of Fuel Cells & Hybrid Power Sources, Dalian Institute of Chemical Physics, Chinese Academy of Sciences, Dalian 116023, *China*

(Received 17 April 2022; revised manuscript received 23 September 2022; accepted manuscript online 7 November 2022)

Proton-exchange membrane fuel cells (PEMFCs) have been widely used commercially to solve the energy crisis and environmental pollution. The oxygen reduction reaction (ORR) at the cathode is the rate-determining step in PEMFCs. Platinum (Pt) catalysts are used to accelerate the ORR kinetics. Pt's scarcity, high cost, and instability in an acidic environment at high potentials seriously hinder the commercialization of PEMFCs. Therefore, studies should explore electrocatalysts with high catalytic activity, enhanced stability, and low-Pt loading. This review briefly introduces the research progress on Pt and Pt-based ORR electrocatalysts for PEMFCs, including anticorrosion catalyst supports, Pt, and Pt-based alloy electrocatalysts. Advanced preparation technology and material characterization of Pt-based ORR electrocatalysts are necessary to improve the performance and corresponding reaction mechanisms.

Keywords: electrocatalysts, oxygen reduction reaction, activity, stability

PACS: 81.05.U–, 81.07.–b, 81.07.Bc, 82.45.Jn **DOI:** 10.1088/1674-1056/aca081

1. Introduction

Proton-exchange membrane fuel cells (PEMFCs) are attracting widespread attention as an alternative to conventional internal combustion engines, secondary batteries, and other energy sources. PEMFCs have become the mainstream choice for vehicle fuel cells owing to their high energy conversion efficiency, low noise, and zero emissions. The research of PEMFCs has achieved great progress, and several demonstrations of PEMFC vehicles have been documented. Some countries, including Japan, the European Union, the United States, and China, have promoted new energy vehicle deployment to national strategies to relieve energy pressure and reduce environmental pollution.

The oxygen reduction reaction (ORR) that occurs at the cathode is a very critical reaction in PEMFCs. As the rate of ORR on the cathode is orders of magnitude slower than that of the hydrogen oxidation reaction on the anode, the cathode requires more platinum (Pt) than the anode to accelerate oxygen reduction.[1,2] The loss of cathode performance due to the slow ORR kinetics is the main reason for the low fuel-cell performance. Although Pt is the most active single-element catalyst for ORR, its rarity, limited reserves, and high price increase the cost of fuel cells and limit their large-scale application. To improve catalyst performance and reduce catalyst cost, researchers focus on two aspects: low-Pt and non-Pt catalysts. In alkaline electrolytes, non-Pt catalysts show fast ORR kinetics and are promising replacement for Pt. However, acidic PEMFCs give better power density and stability than alkaline fuel cells and are more suitable for large-scale industrialization. Meanwhile, the activity and long-term stability of non-Pt catalysts for ORR are still poorer than those of Pt catalysts in acidic environments. Therefore, industrial cathode catalytic materials are mainly Pt-based catalysts.

Under acid and oxygen-enriched environment, industrial Pt/C catalysts show insufficient stability owing to the dissolution and redeposition, migration, and aggregation of Pt nanoparticles (NPs) on carbon supports and the Pt shedding caused by the corrosion of carbon supports.[3] Therefore, the exploration of antioxidant catalyst supports and electrocatalysts with low-Pt content and enhanced stability is critical to promote the commercialization of fuel cells. This paper briefly introduces the research progress of ORR electrocatalyst for PEMFCs from the aspects of catalyst supports, Pt, and Pt alloy electrocatalysts.

2. Catalyst supports

Although Pt catalysts promise higher activity and durability than any other single-metal catalysts, high loading of Pt is required to achieve a high power density due to the large overpotential of Pt catalysts.[4] However, in the absence of support materials, the increase in Pt concentration leads to the aggregation of Pt NPs, reduced surface area, and decreased utilization of Pt.[5] A catalyst support is necessary to achieve highly dispersed Pt NPs with improved Pt utilization and high catalytic performance. Importantly, the interaction between support and catalyst affects the activity and durability of electrocatalysts. In general, catalyst support materials should meet the following criteria:[6] large specific surface area (SSA) for

[†]Corresponding author. E-mail: zhgshao@dicp.ac.cn

© 2022 Chinese Physical Society and IOP Publishing Ltd

the improvement of catalyst dispersion and high electrochemical stability under fuel-cell operating conditions. To date, catalyst supports are mainly based on carbon.

2.1. Carbon black

Carbon black (CB) is the most widely used catalyst support material because of its large surface area, excellent conductivity, porous structure, and low cost.[7] Many kinds of CB, including Vulcan XC-72R, Ketjenblack ECP300J, and Ketjenblack ECP600JD, are available.[8–10] Although the commonly used CB materials show a good performance, they easily corrode at high potentials, which results in the agglomeration and growth of the supported NPs and reduction of electrochemical SSA. Enhancing the graphitization degree of carbon support is an important way to improve stability. Luo *et al.*[11] and Watanabe *et al.*[12] observed that graphitized CB (GCB) support can enhance the corrosion resistance of Pt/GCB at high potential. The stability of Pt/GCB is evidently better than that of ordinary Pt/C catalyst. During the ORR catalytic process, catalysts are susceptible to poisoning under air feed containing traces of SO_x, NO_x, and PO_x contaminants, resulting in the decreased activity and durability of H_2–air fuel cells. According to the literature,[13] P and N dual-doped carbon exhibited an antipoisoning effect with superior structural stability against small molecular poisons.

2.2. Mesoporous carbon

Most breakthroughs in fuel-cell performance have been associated with an increase in the three-phase (catalyst/H^+ conductor–ionomer/O_2) interface. Considering that sulfonate groups in the perfluorosulfonic acid ionomer negatively affect Pt activity, the ionomer cannot be considerably distant from Pt. The internal pores of mesoporous carbon carriers not only can support Pt NPs and protect them from direct adsorption by ionomers but also allow H^+ and O_2 to be accessible to the catalysts. Ramaswamy *et al.*[14] reported that the reduction in the micropore and macropore volumes of the carbon support will favor O_2 transport near the Pt catalyst surface and bulk H^+ transport in the ionomer phase. Yarlagadda *et al.*[15] discussed the mesoporous regions affecting the kinetic property of catalysts. They suggested that porous carbons with a preferred pore opening of 4–7 nm can provide catalysts with excellent ORR activities and transport properties. The above research results indicated that ideal carbon supports should have minimal micro- and macropore regions and appreciable mesopore regions.

The ordered Pt_3Co/C intermetallic catalysts can be obtained by heating the Pt NPs deposited on the carbonized Co-doped ZIF-8.[16] During thermal treatment, the doped Co atoms in the carbon support diffuse and combine with Pt atoms, thus enhancing the interaction between Pt_3Co NPs and the support and improving the catalytic activity and stability. Based on the current research, carbon supports should have high graphitization degree and SSA and show good activity and stability as Pt NP supports. In the synthesized three-dimensional (3D) ordered mesoporous carbon sphere-supported Pt NPs (Pt/OMCS) [Figs. 1(a) and 2(b)], Pt particles with an average size of ~ 1.6 nm were uniformly dispersed on the mesopore walls of the carbon spheres.[17] Compared with CB-supported Pt catalysts, Pt/OMCS catalysts had a smaller Pt particle size, better Pt dispersion, larger electrochemical surface area (ECSA), higher ORR activity, and better electrocatalytic stability [Figs. 1(c) and 1(d)].

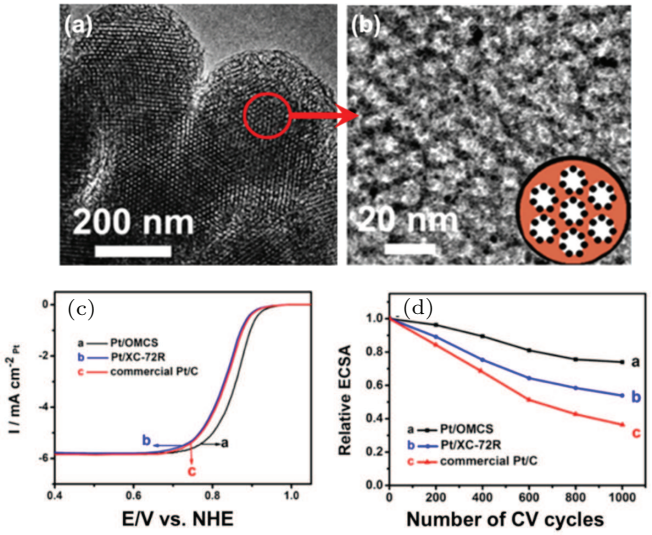


Fig. 1. (a) Transmission electron microscopy (TEM) image and (b) high-resolution TEM (HRTEM) image of Pt/OMCS. (c) ORR curves of the catalysts in O_2-saturated 0.5 M H_2SO_4 solution at room temperature (5 mV·s^{-1}, 1600 rpm). (d) Loss of the ECSA of catalysts with the number of cyclic voltammetry (CV) cycles in Ar-saturated 0.5 M H_2SO_4 solution at room temperature (50 mV·s^{-1}, 0.0–1.3 V vs. RHE).[17]

2.3. Graphene

Compared with other sp^2-bonded carbon materials, graphene has a unique ultrathin sheet structure, ultrahigh SSA, good electrical conductivity, and stable physical properties; thus, it has broad application prospects in the preparation of high-performance fuel-cell catalysts.[18] Graphene has a larger surface area than CB.[19] Currently, various synthetic strategies for preparation of graphene-supported nanocatalysts as ORR catalysts have been investigated.

For instance, Tang *et al.*[20] constructed a novel 3D hierarchical structure with reduced graphene oxide (rGO) and poly dimethyl diallyl ammonium chloride-functionalized CB (FCB) to anchor Pt NPs as an efficient electrocatalyst for PEMFCs. Pt/rGO_1-FCB_2 showed a good 3D interconnected framework by optimizing the weight ratio of rGO/FCB. This unique structure has the advantages of large surface area, ideal porosity, high graphitic crystallinity, and uniform dispersion of ultrafine Pt NPs. Benefiting from unique structural features, the Pt/rGO_1-FCB_2 catalyst showed significantly im-

proved ORR activity and stability compared with the commercial Pt/C. In addition, the electrode assembled with this catalyst exhibited excellent performance in single-cell tests, with a peak power density of 1.344 $W{\cdot}cm^{-2}$ and a maximum mass-specific power density of 7.5 $W{\cdot}mg^{-1}$, which were higher than those of conventional Pt/C electrodes. The stabilities of ECSA, power density, and kinetic resistance during accelerated degradation suggest that the Pt/rGO$_1$-FCB$_2$ electrode exhibits a superior electrochemical durability to the commercial Pt/C. Zhou *et al.*[21] synthesized holey graphene nanosheets (HGN) with a meso-macroporous structure. Pt/HGN-900 showed higher catalytic activity and stability than Pt/XC-72 and Pt/rGO.

2.4. Fe–N–C support materials

Modified carbon supports, such as Fe/N codoped carbon, have been widely used as carriers for supporting Pt-based alloy catalysts owing to their excellent catalytic activity for ORR, high stability, and low cost.[22,23] Li *et al.*[24] used Fe/N-doped activated carbon as a carrier (FeN-C) and loaded it with Pt NPs. The ECSA of commercial Pt/C lost approximately 43% after the aging test, whereas that of Pt/FeN-C catalyst showed no evident change. This finding was observed because the interaction between the surface functional groups of modified support and Pt NPs can prevent the agglomeration of Pt NPs during the test process, which indicated that FeN-C as a support can effectively improve the stability of Pt catalysts in ORR catalysis. Qiao *et al.*[23] reported the Pt NPs with a small size of ~ 2 nm and uniform dispersion on FeN_4 site-rich carbon support (Pt/FeN_4-C). The Pt/FeN_4–C catalyst exhibited a half-wave potential of 30 mV vs. RHE higher than that of Pt/NC in 0.1 M $HClO_4$ electrolyte. After 30000 cycles, the half-wave potential decreased by 10 mV. The superior activity and stability for ORR were mainly due to the synergistic effect of Pt NPs and FeN_4 sites. The dense FeN_4 sites in the carbon support enhanced the interaction between Pt and carbon, which significantly alleviated the agglomeration of NPs and improved the stability of the catalyst. Kuttiyiel *et al.*[25] presented a novel Janus structured catalyst consisting of Pt NPs deposited on Fe–N–C supports for ORR. The ORR activity and durability of the catalyst were improved as the unique Janus structure was further bonded owing to the synergetic effect.

2.5. Noncarbonaceous materials

During the long-term operation of PEMFCs, the carbon support is inevitably corroded, resulting in the loss of fuel-cell performance.[26] Therefore, many noncarbonaceous materials, such as conducting or semiconducting oxides and carbides, and heteroatom-doped diamond, have been developed as catalyst support materials or secondary supports to modify catalyst supports for PEMFCs. This condition not only reduces the loading of noble-metal (NM) electrocatalysts but also improves catalytic activity and stability.

Popov *et al.*[27] reported that the Pt/TiO_2 catalyst has desirable fuel-cell performance and high durability, which are attributed to the low mass transfer limitation of Pt/TiO_2 catalyst and the strong metal–support interaction between Pt particles and TiO_2 support, respectively. The developed boron-doped diamond-stabilized Pt catalysts exhibited no loss in activity after 2000 potential cycles.[28] The surrounding carbon matrix is expected to reduce the mobility of Pt NPs, thereby improving the stability of resultant catalysts. Carbides consist of carbon and a less electronegative element, and most of them show some level of covalent property.[29,30] Nie *et al.*[31] deposited Pt NPs directly on tungsten carbide, which showed considerably higher ORR activity than the Pt/C catalyst. In addition to the promoted catalytic activity, it also exhibited a high durability under fuel-cell operation conditions.

3. Pt catalysts

Except for the selection of suitable support materials to enhance catalytic activity and stability, Pt nanostructures with multidimensional morphologies, which can greatly increase the number of exposed Pt active centers and enhance fuel-cell performance, must be controlled.

3.1. Pt NPs

Pt is widely regarded as the most efficient electrocatalyst for PEMFCs. In general, smaller-sized Pt nanocrystals provide higher ECSA and enhanced catalytic activity than larger-sized Pt nanocrystals. Furthermore, Pt nanocrystals with specific surface structures significantly enhance the electrocatalytic activity toward ORR.[32,33]

The ORR activity of individual Pt NPs was evaluated using a nanocollision electrochemical method to investigate the effect of size on the ORR performance.[34] The size-normalized activity of Pt NPs with a diameter of 4 nm was twice that of 25 nm, which confirmed the finding that intrinsic activity depends on the size of NPs. This work has important implications for understanding the nature of ORR electrocatalysis at the atomic scale and validating the structure–activity correlation. Wang *et al.*[35] synthesized monodispersed 8 nm Pt nanocubes by reducing $Pt(acac)_2$ in the presence of oleic acid, oleylamine, and iron pentacarbonyl. The self-assembly of these nanocubes resulted in a (100) textured array. The results of electrochemical tests carried out in an adsorbing electrolyte (H_2SO_4) showed that the SA of Pt nanocubes was more than twice that of Pt NPs from the commercial Pt/C. This phenomenon was attributed to the different adsorption capabilities of bisulfate anions on the Pt (100) and (111) surfaces,[36] in accordance with the report of Markovic *et al.*[37]

The most advanced ORR electrocatalysts are based on various carbon carriers supported by Pt NPs. However, the typical NP morphologies show a large number of defect sites with a low catalytic activity. These defects decrease the reaction kinetics and durability for long-term application in fuel cells owing to the irreversible oxidation of surface atoms.[38,39] In this case, a promising way to overcome this shortcoming is to control the shape of nanocatalysts. The synthesis of new nanostructured materials is an important topic to optimize existing Pt NP catalysts.

3.2. Pt nanowires

One-dimensional (1D) Pt nanowires (NWs) exhibit increased activity and stability toward ORR. Novel 1D sulfur-doped carbon nanotube (S-CNT)-supported 1D Pt NWs (Pt NW/S-CNT) were prepared using a modified solvothermal method for ORR.[40] The interconnected 3D nano-assemblies of Pt NWs and S-CNT showed a higher electrochemical activity and remarkable long-term stability in contrast to commercial Pt/C. Wang *et al.*[41] prepared Pt NW arrays on sulfur-doped graphene (Pt NW/S-G). The Pt NWs had an ultrathin diameter of 2–5 nm and were densely covered on the surface of the support [Fig. 2(a)]. The structure of the composite can be easily controlled by fine-tuning the nucleation and growth kinetics of Pt NWs and Pt–support interactions. Electrochemical characterization indicated that the ORR activity of the composites was more than twice higher than that of commercial Pt/C. Based on the anomalous size effect of diameter-tunable Pt NWs, the ORR activity and stability monotonically increased as the diameter decreased from 2.4 nm to 1.1 nm[42] [Figs. 2(b)–2(e)]. The experimental results showed that the decrease in NW diameter led to an increase in compressive strain, and this change played a dominant role in weakening the adsorption and suppressing the dissolution of Pt, which confirmed this anomalous size effect. The reduction of low-coordination sites on NWs as an intrinsic structural advantage was the main root of this effect.

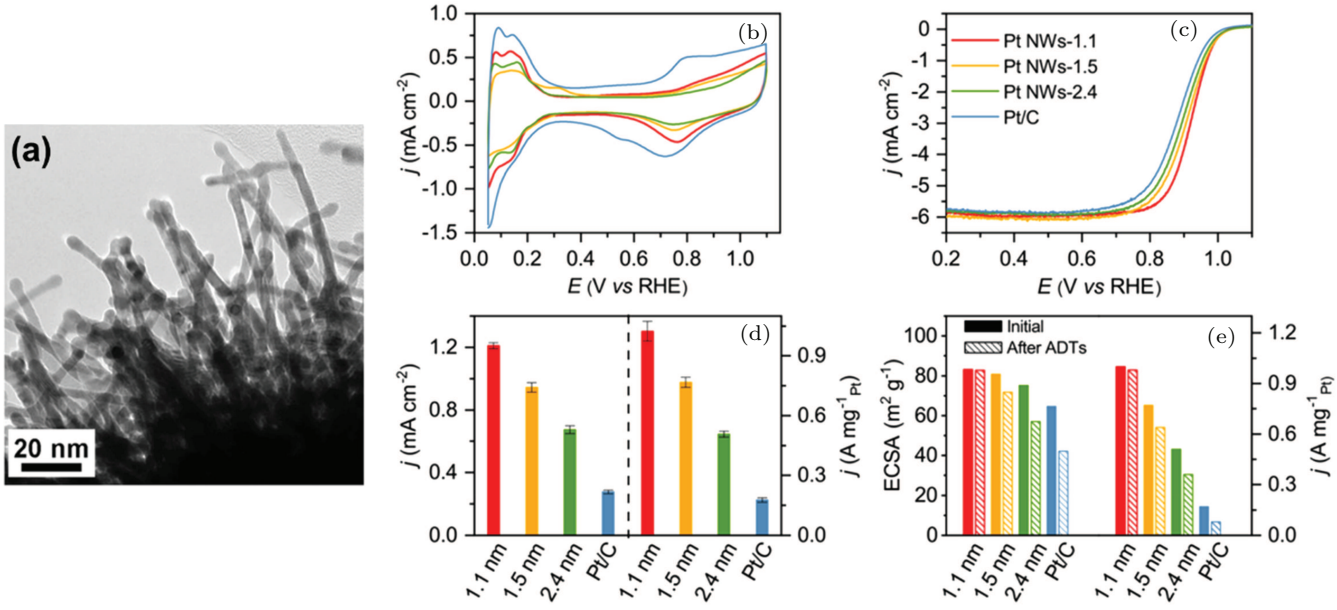


Fig. 2. (a) HRTEM image of Pt NW/S-G catalyst.[41] ORR performance of Pt NWs with different diameters. (b) Cyclic voltammograms recorded in a N_2-purged 0.1 $MHClO_4$ solution with a sweep rate of 50 $mV{\cdot}s^{-1}$. (c) ORR polarization curves recorded in an O_2-purged 0.1 $MHClO_4$ solution with a sweep rate of 10 $mV{\cdot}s^{-1}$ and a rotation rate of 1600 rpm. (d) Comparison of SA and MA at 0.9 V vs. RHE. (e) Changes in the ECSA and MAs before and after 10000 cycles of the accelerated degradation test (ADT).[42]

3.3. Pt nano-frameworks

Metal–organic framework (MOF)-derived materials have received increasing attention in the field of energy storage and conversion. The calcination of MOFs into carbonized structures is a common route to obtaining MOF-derived materials. However, the existing calcination conditions usually lead to structural collapse and a significant reduction in SSA. To avoid the structural collapse during the calcination process, Wang *et al.*[43] introduced hydrogen into the protection gas. ZIF-8 MOFs were calcined in an Ar–H_2 gas mixture to obtain N-doped porous carbon materials (Fig. 3). The obtained sample completely inherited the rhombic dodecahedron shape of precursor ZIF-8. H_2 reduced the Zn in ZIF-8 at high temperatures and assisted the evaporation of metallic Zn, avoiding the carbothermal reduction reaction between the Zn component and carbon skeleton of MOFs, protecting the skeleton of MOFs, and leaving a large number of micropores. Pt NPs were supported on the prepared porous carbon to catalyze ORR. When the Pt loading was 8.66 wt.%, the catalyst showed an excellent half-wave potential of 0.883 V vs. RHE, which was 10 mV higher than that of commercial 20 wt.% Pt/C. The stability was also considerably better than that of Pt/C catalysts.

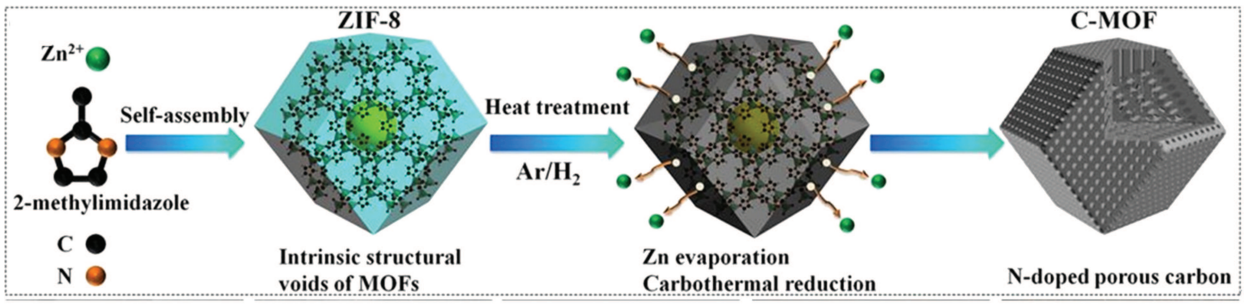


Fig. 3. Schematic of the preparation process of 3D N-doped porous carbon.[43]

Similarly, the confinement of Pt NPs on conjugated nitrogen-rich covalent organic frameworks (COFs) is beneficial for the catalysis of ORR in acidic electrolytes.[44] In the catalyst, multiple pyridine nitrogen as nucleation centers can be used to control the growth of Pt on the surface and pore channel of COFs. As a result, the Pt NPs were uniformly distributed, and the Pt active centers were more accessible. The catalyst showed an ultrahigh ORR performance with an onset potential of 1.05 V vs. RHE and a half-wave potential of 0.89 V, which are superior to those of commercial Pt/C. This strategy provides a new approach to preparing electrocatalysts with atomically defined active centers and high-performance catalytic activity for clean energy storage and conversion.

3.4. Pt single-atom catalysts

The size, shape, composition, and structure of NPs must be controlled reasonably to explore more efficient catalysts. In 2011, the team of academicians and Zhang from the Dalian Institute of Chemical Physics reported the Pt_1/FeO_x single-atom catalyst (SAC) for the first time and, on this basis, proposed the concept of "single-atom catalysis."[45] Since then, the emerging heterogeneous SACs have become a hot spot in the field of catalysis because of their maximum atom utilization, uniform active sites, and excellent activity and selectivity for specific reactions.[46] The development of SACs will greatly expand electrocatalysis research and further promote the development of electrochemical energy conversion and storage technologies.

Carbon-supported high-performance Pt single-atom oxygen reduction electrocatalysts against carbon monoxide/methanol have been reported.[47] The single-cell test results showed a power density of 0.68 $W\cdot cm^{-2}$ and good durability at a Pt loading of 0.09 $mg\cdot cm^{-2}$ at 80 °C. Cho *et al.*[48] prepared Pt single-atom (Pt_1) electrocatalysts with a Pt loading of about 5 wt.% on nitrogen-doped activated carbon (N-doped black pearl, NBP) supports (Pt_1/NBP) for ORR using a hydrothermal ethanol reduction method. Through further high-temperature pyrolysis of Pt_1/NBP, the coordination structure of the isolated Pt atoms was reconstructed to generate unique nitrogen-anchored Pt single atoms (Pt_1@Pt/NBP). A total of 47.8% of isolated Pt atoms and well-dispersed Pt NPs were retained on the carbon supports. As a cathode catalyst for PEMFCs, the MA of Pt_1@Pt/NBP reached 133.3 $A\cdot g_{Pt}^{-1}$ at a cell voltage of 0.9 V, which was 8.7 times that of commercially available Pt/C. The UNSW team[49] believed that the catalytic performance of Pt single-atom site was enhanced by the design of coordination structure, which can improve the reaction selectivity and realize the 4-electron ORR pathway. Therefore, the phosphorus atom with more valence electrons was selected to participate in the construction of Pt-atom active sites. The catalyst successfully synthesized by the researchers contained approximately 0.026 wt.% Pt, but its turnover frequency was as high as 6.80 s^{-1}, which is nearly 170 times that of commercial Pt/C (20 wt.%) at 0.9 V vs. RHE.

4. Pt-based alloy catalysts

In the early research on Pt catalysts and the ORR mechanism, the results showed that the surface of catalysts with excellent performance should have an appropriate adsorption energy for O_2 to promote the cleavage of O=O double bonds and be suitable for the desorption of decomposed products. However, the adsorption energy of O_2 on the surface of pure Pt is extremely large. Thus, Pt must be adjusted to reduce the adsorption energy by approximately 0.2 eV, further improving its catalytic activity. For most transition metals (TMs), their atomic radii are smaller than those of Pt atoms. Doping TM atoms into Pt lattices can cause the latter to shrink and generate stress and change the electronic structure of Pt. Therefore, the catalytic activity toward ORR of the catalysts formed by alloying Pt with TMs has been greatly improved because of the combined geometric and electronic effects. Alloy catalysts can take advantage of the synergy and mutual influence between metals to prevent the agglomeration and exfoliation of Pt. In addition, alloying can increase the oxidation potential of Pt and promote the desorption of O_2 on the surface of Pt, thereby enhancing the stability and ORR activity of the catalysts.

4.1. Binary Pt-based alloys

Carbon-supported ultrathin Pt NWs and Pt_3Ni NWs were synthesized using a soft templating method.[50] Pt_3Ni NWs

catalysts have higher electrocatalytic activity and better stability for ORR than Pt NW and Pt/C catalysts. The improved activity was attributed to the promoted desorption of oxygen-containing species and the release of active sites due to the downshifted-band center of Pt caused by the interaction between Pt and Ni in the alloy. Tang *et al.*[8] successfully prepared Pt-Co/C alloys with four different initial Pt/Co atom ratios using a modified polyol method. The actual atomic ratios of Pt to Co for Pt–Co alloys with initial Pt/Co atom ratios of 4:1, 2:1, 1:1, and 1:2, were 93:1, 82:1, 36:1, and 31:1, respectively. $Pt_{36}Co/C$ catalyst exhibited the best ORR performance among all Pt-Co/C and commercial Pt/C catalysts, with a half-wave potential of 0.884 mV, ECSA of 90.6 $m^2 \cdot g^{-1}$, SA of 0.258 $mA \cdot cm^{-2}$ (at 0.9 V_{RHE}), and MA of 0.233 $A \cdot mg^{-1}$ (at 0.9 V_{RHE}). According to the ECSA and MA values obtained ([Fig. 4(d)] from the CV and linear scanning voltammetry (LSV) data in Figs. 4(a)–4(c), the $Pt_{36}Co/C$ catalyst possessed better durability than commercial Pt/C. Sun *et al.*[51] synthesized Pt_3Cu icosahedron via a solvothermal method using hexadecyl trimethyl ammonium bromide as the morphology control agent. The ECSAs of Pt_3Cu icosahedron and octahedron were 34.4 $m^2 \cdot g^{-1}$ and 31.5 $m^2 \cdot g^{-1}$, respectively, which were more than twice that of the Pt/C (15.1 $m^2 \cdot g^{-1}$). The prepared carbon-supported ultrathin Pt shell-encapsulated Pd NP catalyst (Pd@Pt/C)[52] exhibited significantly improved ECSA, electrocatalytic activity, and NM utilization. The ECSA, area-specific activity, and NM-/Pt mass-specific activity were 1.3, 2.4, and 1.9/3.1 times those of commercial Pt/C, respectively. Moreover, the catalyst showed a good electrochemical stability during the ADT. The ORR high performance benefited from the ultrathin Pt shell nanostructure and the resulting ligand and geometric effects. Liu *et al.*[53] synthesized Pt–Ru alloy catalysts and observed that the Pt/Ru molar ratio was positively correlated with the ORR activity but negatively correlated with SO_2 tolerance. In particular, the SO_2-tolerant catalyst with a Pt/Ru molar ratio of 6:1 showed a competitive initial MA of 0.287 $A \cdot mg_{Pt}^{-1}$ and maintained 60% MA after SO_2 poisoning, which were considerably higher than those of commercial Pt/C (0.27 $A \cdot mg_{Pt}^{-1}$ and 30%, respectively). The presence of Ru changed the interaction between Pt and SO_2 for antipoisoning performance improvement. The Ru incorporation strategy is expected to improve the SO_2 tolerance of other most advanced Pt-based alloy catalysts. Other binary alloy catalysts, such as Pt–Ir and Pt–Au,[54–56] that showed remarkable ORR activity and enhanced stability have been studied.

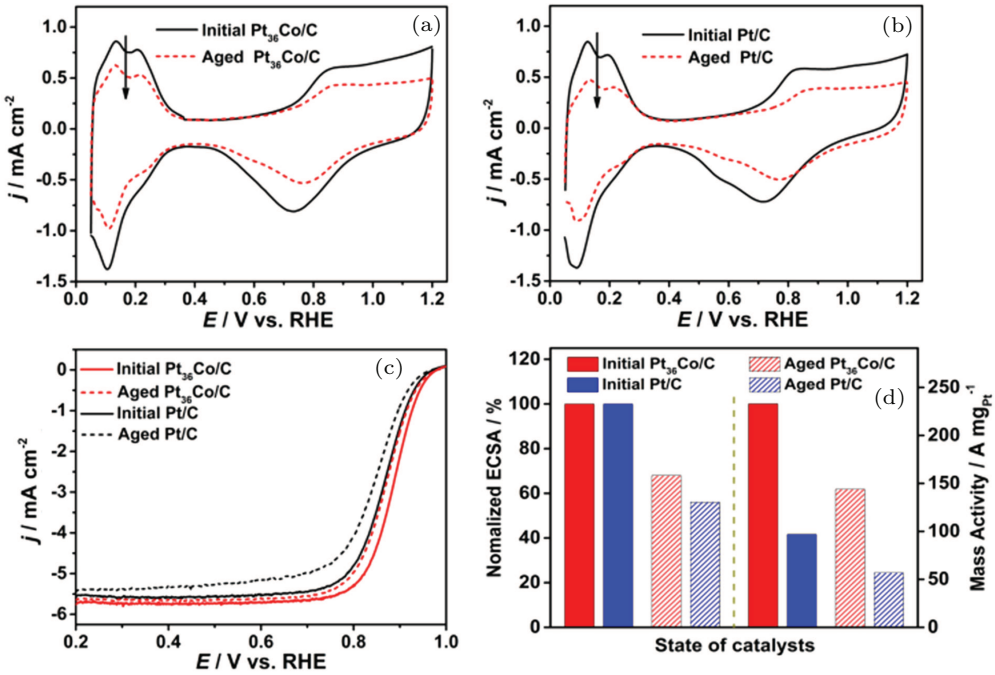


Fig. 4. CV curves of (a) $Pt_{36}Co/C$ and (b) commercial Pt/C before and after 1500 cycles; (c) LSV polarization curves and (d) ECSA and MA of $Pt_{36}Co/C$ and Pt/C before and after 1500 cycles.[8]

To improve and optimize ORR performance and stability in PEMFCs, scientists envisioned fields beyond Pt-based disordered alloys. The researchers described a new class of Pt-Co nanocatalysts consisting of an ordered Pt_3Co intermetallic core and a Pt shell that is two to three atomic layers thick.[57] The MA and SA of these nanocatalysts increased by more than 200% and 300%, respectively, compared with those of the disordered Pt_3Co alloy NPs and Pt/C. Thus far, the MA of ORR is the highest among the Pt–Co systems reported in the literature under similar test conditions. The activity loss after 5000 potential cycles is minimal, and the ordered core–shell structure remains nearly intact. The high activity and stability are attributed to the Pt-rich shell and stable intermetallic Pt_3Co core. These ordered NPs provide a new research direction for per-

formance optimization of next-generation PEMFCs. Carbon-supported structurally ordered Pt_3Mn intermetallic NPs without severe agglomeration exhibited highly active and stable ORR.[58] The single-cell using the Pt_3Mn intermetallic/C cathode catalyst achieved a high current density of 0.550 A·cm^{-2} at a cell voltage of 0.7 V and stability (−11.63%) after 10 K voltage cycles, which are superior to those of commercial Pt/C (0.419 A·cm^{-2} and −26.49%, respectively). For N-doped carbon shell-clad Pt–Fe intermetallic NPs,[59] the literature showed that the N-doped carbon shell not only prevented the agglomeration of NPs but also facilitated the uniform distribution of NPs on the carbon support. The catalyst exhibited excellent ORR activity and stability and enhanced antitoxicity to SO_x and PO_x. Besides the catalysts mentioned above, Pt-based binary intermetallic compounds, such as Pt_3In and Pt_3Sn,[10,60] have been reported.

4.2. Ternary Pt-based alloys

Compared with binary Pt alloys, ternary Pt alloys generally allow for greater flexibility to tune the electronic structure and catalytic properties of Pt.[61,62] In recent experiments, Pt ternary alloys achieved ordered transformation more easily than Pt binary alloys. For example, the addition of a small amount of Cu can effectively reduce the temperature required for structural ordering of Pt–Fe alloys.[63,64] Co can also enhance the ordering of Pt–Ni–Co alloys compared with Pt–Ni alloys.[65] Therefore, structurally ordered Pt ternary intermetallic compounds for ORR have attracted extensive interest.

The carbon-supported Mo-doped Pt_3Ni octahedra showed the best ORR performance with a SA of 10.3 mA·cm^{-2} and a MA of 6.98 A·mg$_{Pt}^{-1}$, which were 81- and 73-fold enhancements compared with those of commercial Pt/C catalysts (0.127 mA·cm^{-2} and 0.096 A·mg$_{Pt}^{-1}$, respectively).[66] Theoretical calculations suggest that Mo prefers subsurface positions near the particle edges in vacuum and surface vertex/edge positions under oxidation conditions, where it enhances the performance and stability of the Pt_3Ni catalyst. The carbon-supported Mo-doped PtFe (Mo–PtFe/C) NPs manifested distinct improvement in ORR activity compared with commercial JM Pt/C catalyst in an acidic medium.[67] The exceptional ORR catalysis of Mo–PtFe/C originated from the increased amount of catalytically active sites of small-sized intermetallic NPs and the optimally weakened oxygen binding energy tuned by Mo. The highly stable and active Mo–PtCu/C displayed twofold and fourfold higher ORR half-cell kinetics than the reference PtCu/C and Pt/C.[68] Electrochemical-accelerated stability tests revealed that dealloying was greatly reduced in Mo–PtCu/C in contrast to the binary alloys PtCu/C and PtMo/C. The exceptional stability of Mo–PtCu can be attributed to the oxidative resistance of Mo-doped atoms. The rationally designed Mo–PtPd@Pt core–shell octahedron has unique compositional advantages, including the segregation of Mo atoms on the vertices and edges and the two to three shell layers of Pt atoms on the surface of the PdPt alloy core, which can provide high activity sites for ORR catalysts and improve electrochemical stability.[69]

Wang *et al.*[70] studied the annealing-induced structural ordering transformation of three Pt-based ternary alloys (PtFeCo, PtNiCo, and PtFeNi). Fe atoms can significantly promote the structural ordering due to their fast atomic diffusion, and Co atoms can effectively suppress the alloy NP sintering. Therefore, the synergistic effect of Co and Fe cannot only achieve a high ordering degree but also inhibit the severe NP agglomeration caused by annealing. The PtFeCo catalyst containing Co and Fe exhibited the highest ordering degree and a minimal NP growth after high-temperature treatment at 600 °C, giving rise to the highest ORR activity and the best stability under acidic conditions. The MA of 0.65 A·mg$_{Pt}^{-1}$ at 0.9 V was four-fold higher than that of pure Pt, and it decreased by 16% after 10000 potential cycles (Fig. 5). The membrane electrode assemblies were prepared using a decal transfer method with Pt/C, Pt–Co/C, and PtCoMn/C as cathode catalysts.[71] The R_{ct} value of PtCoMn/C-based electrode at the rate voltage of 0.68 V was the smallest, which indicated that the ORR catalytic activity of PtCoMn/C was higher than that of the other two catalysts [Fig. 6(a)]. The power density of PtCoMn/C-based electrode with an ultralow Pt loading of 0.147 mg·cm^{-2} was 1.42 W·cm^{-2}, which was 340 mW·cm^{-2} higher than that of MEA-Pt/C with a resemblant Pt loading [Fig. 6(b)]. The effect of composition and surface structure of single-crystal Pt–Pd–Co ternary alloy electrodes on the ORR activity was investigated by Torihata *et al.*[72] The activity on $Pt_{45}Pd_{45}Co_{10}$ [$Pt_{45}Pd_{45}Co_{10}(100) \approx Pt_{45}Pd_{45}Co_{10}$ (111) < $Pt_{45}Pd_{45}Co_{10}$ (110)] was different from that on $Pt_{77}Pd_8Co_{15}$ [$Pt_{77}Pd_8Co_{15}$ (100) < $Pt_{77}Pd_8Co_{15}$ (110) < $Pt_{77}Pd_8Co_{15}$ (111)]. The specific activities of $Pt_{45}Pd_{45}Co_{10}$(110) and $Pt_{77}Pd_8Co_{15}$ (111) were more than twice that of Pt_3Co.

Carbon-supported Pt monolayer shell-coated Cu_1Pd_1 nanospheres with a composition-grade structure were synthesized by Luo *et al.*,[73] and they exhibited significantly enhanced acidic ORR activity and durability. The reasons for these findings can be summarized as follows: (1) the composition-grade structure of Cu_1Pd_1 nanospheres, Cu-induced geometry and ligand effects, and annealing effect; (2) the special structure of the Pt shell (which greatly reduced the Pt loading and maximized Pt utilization); and (3) the synergistic effect of Cu_1Pd_1 core on the Pt shell.

In addition, PtCoNi,[61] PtFeAu,[74,75] and PtFeCu[76,77] ternary intermetallic compounds as ORR electrocatalysts showed higher catalytic activity and stability than other alloys with disordered structures. This finding is related to the electronic and geometric effects introduced by third-element doping and ordered intermetallic structure.

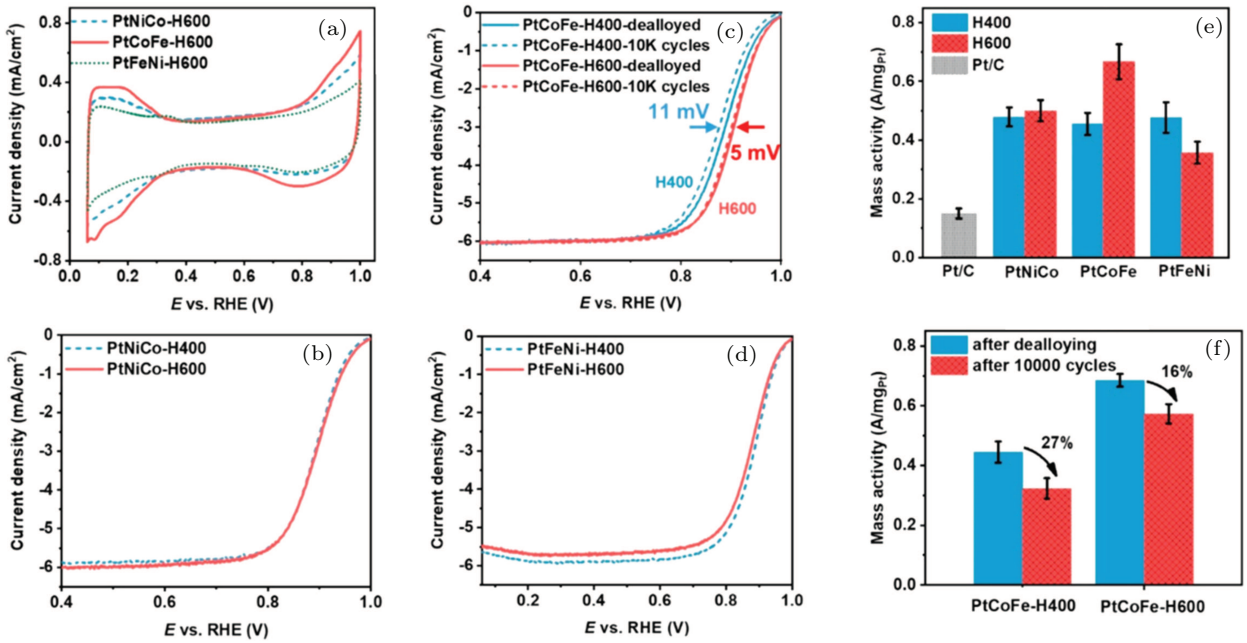


Fig. 5. (a) CV curves of three Pt-based ternary alloys annealed at 600 °C; (b)–(d) LSV polarization curves of PtNiCo, PtCoFe, and PtFeNi, respectively; (e) mass activities of Pt-based ternary alloys and Pt/C; and (f) stability of PtCoFe annealed at 400 °C and 600 °C.[70]

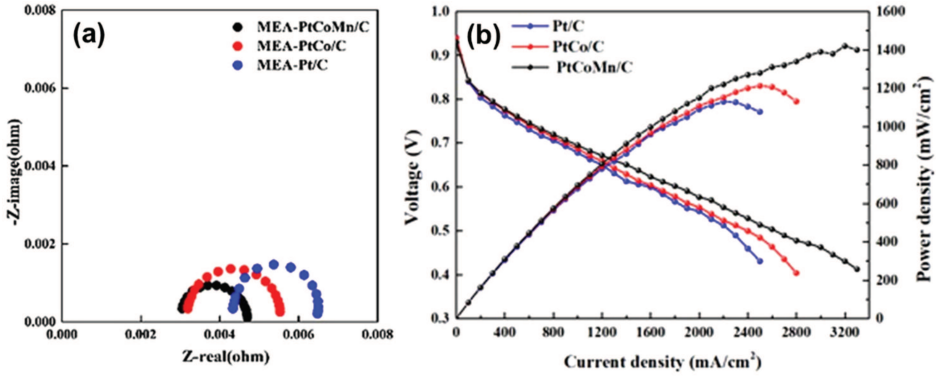


Fig. 6. (a) Electrochemical impedance spectroscopy at 0.68 V and (b) polarization curves before and after IR-free of PtCoMn/C-, Pt-Co/C-, and Pt/C-based electrodes.[71]

4.3. High-entropy Pt-based alloys

Unlike traditional alloys, which are mainly based on one main element, high-entropy alloys (HEAs) contain five or more main elements with similar atomic ratios.[78,79] Great progress has also been made in nanoscale HEAs. By maximizing their surface-to-volume ratio, the application of HEAs have been extended to areas, such as catalysis and energy storage.

Chen *et al.*[80] prepared PtRuCuOsIr nanoporous HEA (np-HEA) catalysts with a 3D bicontinuous ligament/channel structure of approximately 2.5 nm in length using a top-down alloying–dealloying synthetic technique, achieving 1.8- and 3.8-fold enhancement of the MA and SA, respectively, toward ORR than commercial Pt/C and excellent long-term stability. The AlCuNiPtMn np-HEA catalyst with nanoscale face-centered cubic phase structure, which was obtained using the same synthesis method, also exhibited a high half-wave potential of 0.945 V in acidic media and a MA of ∼ 16% for Pt/C.[81] The PtPdFeCoNiHEA NPs were fabricated by means of high-temperature injection.[82] Given the high entropy, lattice distortion, and slow diffusion effects of HEA, the catalyst exhibited superior ORR catalytic activity and electrochemical cycling durability. The MA (1.23 $A \cdot mg_{Pt}^{-1}$) and SA (1.80 $mA \cdot cm_{Pt}^{-2}$) of PtPdFeCoNi HEA were 6.2 and 4.9 times those of Pt/C catalysts, and the half-wave potential was negatively shifted by 6 mV after 50k electrochemical cycles.

5. Summary and perspective

Reducing Pt loading is a medium and long-term solution for the large-scale commercial application of PEMFCs, but the catalytic activity and stability toward ORR still need to be further improved. Different catalyst compositions, structures, and morphologies can facilitate the exposure and stabilization of active sites, thereby enhancing the activity and stability of catalysts. The optimized high SSA and electronic effect can synergistically improve the catalytic efficiency. However, some difficulties in the development of anticorrosion and antipoi-

soning support materials and precise control of microstructure and composition of Pt-based alloy catalysts (disordered, ordered intermetallic, and HEAs), including antiairborne contaminant poisoning ones, must be addressed. In addition, the huge challenge for Pt-based intermetallic compounds, that is, high annealing temperature and long treatment time during synthesis, will promote the ordered structure but lead to significant particle growth. Thus, in maintaining small particle size and intermetallic structure, trade-off issues involving activity and stability should be considered.

Several new prospects are given for the following future directions:

(1) Quantum chemical calculations are used to explore whether a carrier has an anchoring effect on alloy NPs, that is, whether a coupling relationship exists between them. This strategy may provide a new direction for the design of advanced catalysts for PEMFCs.

(2) Novel structures and compositions are the latest development directions of ORR catalysts, and the reasons for their enhanced ORR activity should be comprehensively investigated. The composition–structure–function relationship in the catalytic mechanism should be explored for the rational design and preparation of highly active and durable ORR electrocatalysts.

(3) To understand the mechanism of ORR electrocatalysis from an atomic-scale perspective based on first principles, scientists should consider dynamic simulations on electrocatalytic interfaces. This research work presents great challenges and many opportunities.

(4) In view of the high cost and low reserves of Pt, besides reducing the usage of Pt, attention should be focused on the recovery of Pt.

The continuous progress of preparation technology, material characterization, and deepening of the theoretical research of Pt-based catalysts for ORR will promote the commercialization of fuel cells.

Acknowledgements

Project supported by the National Key Research and Development Program of China (Grant No. 2018YFB1502503) and Strategic Priority Research Program of the Chinese Academy of Sciences (Grant No. XDA21090101).

References

[1] Yang L, Cheng D J, Xu H X, Zeng X F, Wan X, Shui J L, Xiang Z H and Cao D P 2018 *Proc. Natl. Acad. Sci. USA* **115** 6626
[2] Gasteiger H A, Panels J E and Yan S G 2004 *J. Power Sources* **127** 162
[3] Tang R, Wei Z D and Shao Z G 2009 *Battery Bimonthly* **39** 44
[4] Yu X and Ye S 2007 *J. Power Sources* **172** 133
[5] Jung N, Chung D Y, Ryu J, Yoo S J and Sung Y E 2014 *Nano Today* **9** 433
[6] Shao Y Y, Liu J, Wang Y and Lin Y H 2009 *J. Mater. Chem.* **19** 46
[7] Luo Y and Alonso-Vante N 2015 *Electrochim. Acta* **179** 108
[8] Tang X J, Fang D H, Qu L J, Xu D Y, Qin X P, Qin B W, Song W, Shao Z G and Yi B L 2019 *Chin. J. Catal.* **40** 504
[9] Li J R, Sharma S, Liu X M, Pan Y T, Spendelow J S, Chi M F, Jia Y K, Zhang P, Cullen D A, Xi Z, Lin H H, Yin Z Y, Shen B, Muzzio M, Yu C, Kim Y S, Peterson A A, More K L, Zhu H Y and Sun S H 2019 *Joule* **3** 124
[10] Wang Q, Zhao Z L, Zhang Z, Feng T L, Zhong R Y, Xu H, Pantelides S T and Gu M 2020 *Adv. Sci.* **7** 1901279
[11] Luo X, Hou Z J, Ming P W, Shao Z G and Yi B L 2008 *Chin. J. Catal.* **29** 330
[12] Watanabe M, Yano H, Uchida H and Tryk D A 2018 *J. Electroanal. Chem.* **819** 359
[13] Najam T, Shah S S A, Ding W, Jiang J X, Jia L, Yao W, Li L and Wei Z D 2018 *Angew. Chem. Int. Ed. Engl.* **57** 15101
[14] Ramaswamy N, Gu W B, Ziegelbauer J M and Kumaraguru S 2020 *J. Electrochem. Soc.* **167** 064515
[15] Yarlagadda V, Carpenter M K, Moylan T E, Kukreja R S, Koestner R K, Gu W B, Thompson L and Kongkanand A 2018 *ACS Energy Lett.* **3** 618
[16] Wang X X, Hwang S, Pan Y T, Chen K, He Y H, Karakalos S, Zhang H G, Spendelow J S, Su D and Wu G 2018 *Nano Lett.* **18** 4163
[17] Zhang C W, Xu L B, Shan N N, Sun T T, Chen J F and Yan Y S 2014 *ACS Catal.* **4** 1926
[18] Sun Y Q, Wu Q and Shi G Q 2011 *Energy Environ. Sci.* **4** 1113
[19] Antolini E 2012 *Appl. Catal. B* **123–124** 52
[20] Tang X J, Zeng Y C, Cao L S, Yang L M, Wang Z Q, Fang D H, Gao Y Y, Shao Z G and Yi B L 2018 *J. Mater. Chem. A* **6** 15074
[21] Zhou L H, Wang Y X, Tang J, Li J X, Wang S L and Wang Y 2017 *Micropor. Mesopor. Mater.* **247** 116
[22] Liu S W, Li C Z, Zachman M J, *et al.* 2022 *Nat. Energy* **7** 652
[23] Qiao Z, Wang C Y, Li C Z, Zeng Y C, Hwang S, Li B Y, Karakalos S, Park J, Kropf A J, Wegener E C, Gong Q, Xu H, Wang G F, Myers D J, Xie J, Spendelow J S and Wu G 2021 *Energy Environ. Sci.* **14** 4948
[24] Li M H, Yang Z, Pan T X, Tong X, Hu C G and Tian J 2022 *J. Mater. Eng.* **50** 132
[25] Kuttiyiel K A, Sasaki K, Park G G, Vukmirovic M B, Wu L J, Zhu Y M, Chen J G G and Adzic R 2017 *Chem. Commun.* **53** 1660
[26] Wang Y J, Wilkinson D P and Zhang J 2011 *Chem. Rev.* **111** 7625
[27] Huang S Y, Ganesan P, Park S and Popov B N 2009 *J. Am. Chem. Soc.* **131** 13898
[28] Wang J and Swain G M 2003 *J. Electrochem. Soc.* **150** E24
[29] Antolini E and Gonzalez E R 2009 *Solid State Ionics* **180** 746
[30] Lv H F, Peng T, Wu P, Pan M and Mu S C 2012 *J. Mater. Chem.* **22** 9155
[31] Nie M, Shen P K, Wu M, Wei Z D and Meng H 2006 *J. Power Sources* **162** 173
[32] Zhong C J, Luo J, Fang B, Wanjala B N, Njoki P N, Loukrakpam R and Yin J 2010 *Nanotechnology* **21** 062001
[33] Xia B Y, Ng W T, Wu H B, Wang X and Lou X W D 2012 *Angew. Chem. Int. Ed.* **51** 7213
[34] Xiang Z P, Tan A D, Fu Z Y, Piao J H and Liang Z X 2020 *J. Energy Chem.* **49** 323
[35] Wang C, Daimon H, Lee Y, Kim J and Sun S H 2007 *J. Am. Chem. Soc.* **129** 6974
[36] Marković N M, Adžić R R, Cahan B D and Yeager E B 1994 *J. Electroanal. Chem.* **377** 249
[37] Marković N M, Gasteiger H A and Ross Jr P N 1995 *J. Phys. Chem.* **99** 3411
[38] Yu X and Ye S 2007 *J. Power Sources* **172** 145
[39] Shao Y, Yin G and Gao Y 2007 *J. Power Sources* **171** 558
[40] Hoque M A, Hassan F M, Jauhar A M, Jiang G P, Pritzker M, Choi J Y, Knights S, Ye S Y and Chen Z W 2018 *ACS Sustainable Chem. Eng.* **6** 93
[41] Wang R Y, Higgins D C, Hoque M A, Lee D U, Hassan F and Chen Z W 2013 *Sci. Rep.* **3** 2431
[42] Yao Z Y, Yuan Y L, Cheng T, Gao L, Sun T L, Lu Y F, Zhou Y G, Galindo P L, Yang Z L, Xu L, Yang H and Huang H W 2021 *Nano Lett.* **21** 9354
[43] Wang C, Wang X D, Lai F Y, Liu Z, Dong R H, Li W, Sun H X and Geng B Y 2020 *ACS Appl. Nano Mater.* **3** 5698
[44] Zhai L P, Yang S, Yang X B, Ye W Y, Wang J, Chen W H, Guo Y, Mi L W, Wu Z J, Soutis C, Xu Q and Jiang Z 2020 *Chem. Mater.* **32** 9747
[45] Qiao B T, Wang A Q, Yang X F, Allard L F, Jiang Z, Cui Y T, Liu J Y, Li J and Zhang T 2011 *Nat. Chem.* **3** 634

[46] Zhu C Z, Fu S F, Shi Q R, Du D and Lin Y 2017 *Angew. Chem. Int. Ed. Engl.* **56** 13944

[47] Liu J, Jiao M G, Lu L L, Barkholtz H M, Li Y P, Wang Y, Jiang L H, Wu Z J, Liu D J, Zhuang L, Ma C, Zeng J, Zhang B S, Su D S, Song P, Xing W, Xu W L, Wang Y, Jiang Z and Sun G Q 2017 *Nat. Commun.* **8** 15938

[48] Liu J, Bak J, Roh J, Lee K S, Cho A, Han J W and Cho E 2021 *ACS Catal.* **11** 466

[49] Zhu X F, Tan X, Wu K H, Haw S C, Pao C W, Su B J, Jiang J J, Smith S C, Chen J M, Amal R and Lu X Y 2021 *Angew. Chem. Int. Ed.* **60** 21911

[50] Zhang H J, Zeng Y C, Cao L S, Yang L M, Fang D H, Yi B L and Shao Z G 2017 *Front. Energy* **11** 260

[51] Sun X H, Jiang K Z, Zhang N, Guo S J and Huang X Q 2015 *ACS Nano* **9** 7634

[52] Luo L X, Fu C H, Wu A M, Zhuang Z C, Zhu F J, Jiang F L, Shen S Y, Cai X Y, Kang Q, Zheng Z F, Hu C Y, Yin J W, Xia G F and Zhang J L 2022 *Nano Res.* **15** 1892

[53] Liu Y X, Du L, Kong F P, Han G K, Gao Y Z, Du C Y, Zuo P J and Yin G P 2019 *ACS Sustain. Chem. Eng.* **8** 1295

[54] Zhang G, Shao Z G, Lu W T, Li G F, Liu F Q and Yi B L 2012 *Electrochem Commun.* **22** 145

[55] Park J Y, Park H S, Han S B, Kwak D H, Won J E, Lim T and Park K W 2019 *J. Ind. Eng. Chem.* **77** 105

[56] Park H Y, Jeon T Y, Jang J H, Yoo S J, Choi K H, Jung N, Chung Y H, Ahn M, Cho Y H, Lee K S and Sung Y E 2013 *Appl. Catal. B* **129** 375

[57] Wang D L, Xin H L L, Hovden R, Wang H S, Yu Y C, Muller D A, Disalvo F J and Abruña H D 2013 *Nat. Mater.* **12** 81

[58] Lim J, Jung C, Hong D, Bak J, Shin J, Kim M, Song D, Lee C, Lim J, Lee H, Lee H M and Cho E 2022 *J. Mater. Chem. A* **10** 7399

[59] Hu Y Z, Shen T, Zhao X R, Zhang J J, Lu Y, Shen J, Lu S F, Tu Z K, Xin H L L and Wang D L 2020 *Appl. Catal. B* **279** 119370

[60] Rong H P, Mao J J, Xin P Y, He D S, Chen Y J, Wang D S, Niu Z Q, Wu Y and Li Y D 2016 *Adv. Mater.* **28** 2540

[61] Wang C, Li D G, Chi M F, Pearson J, Rankin R B, Greeley J, Duan Z Y, Wang G F, van der Vliet D, More K L, Markovic N M and Stamenkovic V R 2012 *J. Phys. Chem. Lett.* **3** 1668

[62] Zhang S, Zhang X, Jiang G M, Zhu H Y, Guo S J, Su D, Lu G and Sun S H 2014 *J. Am. Chem. Soc.* **136** 7734

[63] Chen L, Bock C, Mercier P H J and MacDougall B R 2012 *Electrochim. Acta* **77** 212

[64] Zhu J, Yang Y, Chen L X, Xiao W P, Liu H F, Abruña H D and Wang D L 2018 *Chem. Mater.* **30** 5987

[65] Wang T Y, Liang J S, Zhao Z L, Li S Z, Lu G, Xia Z C, Wang C, Luo J H, Han J T, Ma C, Huang Y H and Li Q 2019 *Adv. Energy Mater.* **9** 1803771

[66] Huang X Q, Zhao Z P, Cao L, Chen Y, Zhu E B, Lin Z Y, Li M F, Yan A M, Zettl A, Wang Y M, Duan X F, Mueller T and Huang Y 2015 *Science* **348** 1230

[67] He C M, Ma Z L, Wu Q, Cai Y Z, Huang Y G, Liu K, Fan Y J, Wang H Q, Li Q Y, Qi J H, Li Q K and Wu X W 2020 *Electrochim. Acta* **330** 135119

[68] Luo Y, Kirchhoff B, Fantauzzi D, Calvillo L, Estudillo-Wong L A, Granozzi G, Jacob T and Alonso-Vante N 2018 *ChemSusChem* **11** 193

[69] Cho K Y, Yeom Y S, Seo H Y, Kumar P, Lee A S, Baek K Y and Yoon H G 2017 *ACS Appl. Mater. Interfaces* **9** 1524

[70] Wang Z X, Yao X Z, Kang Y Q, Xia D S and Gan L 2019 *Catalysts* **9** 569

[71] Liu S C, Li S, Wang R Y, Rao Y, Zhong Q, Hong K and Pan M 2019 *J. Electrochem. Soc.* **166** F1308

[72] Torihata M, Nakamura M, Todoroki N, Wadayama T and Hoshi N 2021 *Electrochem. Commun.* **125** 107007

[73] Luo L X, Fu C H, Shen S Y, Zhu F J and Zhang J L 2020 *J. Mater. Chem. A* **8** 22389

[74] Zhang S, Guo S J, Zhu H Y, Su D and Sun S H 2012 *J. Am. Chem. Soc.* **134** 5060

[75] Zhu H, Cai Y Z, Wang F H, Gao P and Cao J D 2018 *ACS Appl. Mater. Interfaces* **10** 22156

[76] Sasaki K, Naohara H, Choi Y M, Cai Y, Chen W F, Liu P and Adzic R 2012 *Nat. Commun.* **3** 1115

[77] Arumugam B, Tamaki T and Yamaguchi T 2015 *ACS Appl. Mater. Interfaces* **7** 16311

[78] Miracle D B and Senkov O N 2017 *Acta Mater.* **122** 448

[79] Zhang Y, Zuo T T, Tang Z, Gao M C, Dahmen K A, Liaw P K and Lu Z P 2014 *Prog. Mater. Sci.* **61** 1

[80] Chen X T, Si C H, Gao Y L, Frenzel J, Sun J Z, Eggeler G and Zhang Z H 2015 *J. Power Sources* **273** 324

[81] Li S Y, Tang X W, Jia H L, Li H L, Xie G Q, Liu X J, Lin X and Qiu H J 2020 *J. Catal.* **383** 164

[82] Yu Y N, Xia F J, Wang C J, Wu J S, Fu X B, Ma D S, Lin B C, Wang J A, Yue Q and Kang Y J 2022 *Nano Res.* **15** 7868